RELIABILITY ENHANCEMENT HYBRID SENSING SCHEME FOR SPIN-TRANSFER-TORQUE MRAM

[1]FEI LI, [2]AARTHY MANI, [3]SUNNY Y. H. LUA

[1,2]Institute of Microelectronics, Agency for Science, Technology and Research (A*STAR), 2 Fusionopolis Way, #08-02 Innovis Tower, Singapore 138634
[3]Data Storage Institute, Agency for Science, Technology and Research (A*STAR), 2Fusionopolis Way, #08-01Innovis Tower, Singapore 138634
Email: li_fei@ime.a-star.edu.sg

Abstract - A novel hybrid sensing scheme with enhanced reliability for Spin-Transfer-Torque MRAM (STT-MRAM) was proposed. The sensing scheme performs a mid-point reference read and a grey zone (GZ) cell detection process where a STT-MRAM cell is determined if it falls within the resistance overlapping zone. Based on the detection outcome, weak cells within the GZ that are highly susceptible to read error will undergo a second process variation tolerant non-destructive self-reference sensing (NSRS). Monte-Carlo simulation across process variation and read currents corners demonstrate the enhanced read reliability in the proposed sensing scheme with an average of 44.7%, 92.2% and 95.3% improvement of bit error rate (BER) over the conventional mid-point reference sensing technique with 5%, 8% and 10% standard deviation of the MTJ diameter, respectively. With an extended GZ detection range, the respective BER can be further reduced by 91.3%, 87.7% and 82.3%.

Index Terms - Bit Error Rate, Hybrid Sensing, Monte-Carlo Process Variation, Resistance Overlapping, Stt-Mram, Self-Reference Sensing.

I. INTRODUCTION

High speed performance, low power consumption, promising scalability and almost unlimited programming endurance are amongst the key features of the new generation non-volatile memory: spin-transfer torque magnetic random access memory (STT-MRAM). It has the potential to become the next generation universal memory replacement [1]-[3]. The key storage element of STT-MRAM is magnetic tunneling junction (MTJ) which consists of two ferromagnetic layers (free layer and reference layer), sandwiching a tunneling dielectric film in between. Currently, the most popular choice of the tunneling thin film is magnesium oxide (MgO) due to its high tunneling magnetoresistance [4], [5]. Depending on the direction of current flow through MTJ, the magnetization of the free layer can be set to be parallel or anti-parallel configuration with respect to the reference layer. Therefore, the MTJ exhibits two resistance states Rap and Rp that represent logic states '1' and '0', respectively. Many successful demonstrations of this technology integrated with advanced CMOS process have been reported [2], [6]-[8]. Recent trend sees a push for higher tunneling resistance ration (TMR) to broaden the memory window to improve the yield of the chip [7], [8].

The MTJ diameter and MgO thickness have been identified as two key parameters that affect the resistance distribution of MTJ [9], [10]. As MTJ size shrinks down to 20 nm and smaller [11], [12], process variation becomes more profound [13] and it is more challenging to optimize the material design to achieve a high TMR due to the low resistance area (RA) requirement [12]. Moreover, process induced variation further broadens MTJ resistance distribution [14].

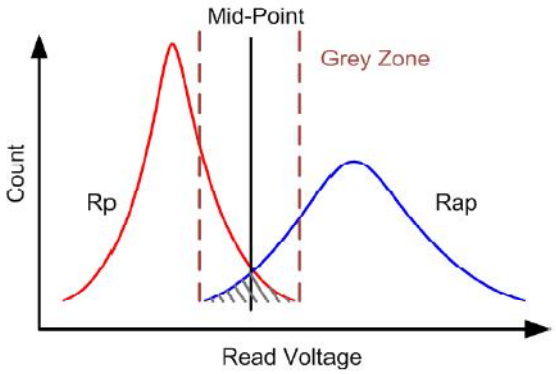

Fig 1. The existence of read voltage grey zone caused by the overlapping of resistance distribution curves.

Under the effect of process variation, the overlapping of resistance distribution could happen as shown in Fig. 1. A cell whose resistance falls within the overlapping zone could either be at its high or low resistance state, therefore its resistance state becomesindistinguishable in the conventional mid-point sensing scheme. Non-destructive self-reference sensing (NSRS) [15] has been proposed as a solution to MTJ cell-to-cell variation at the cost of higher read latency resulted from two read cycles. In the presence of inter-lot and inter-die variations, it is not optimal to employ such a scheme to chips where the effect of resistance overlapping is controlled and can be corrected by simple error-correction-code (ECC) [8]. It is therefore essential to propose a hybrid sensing scheme that activates special variation tolerant

sensing techniques such as NSRS when required.

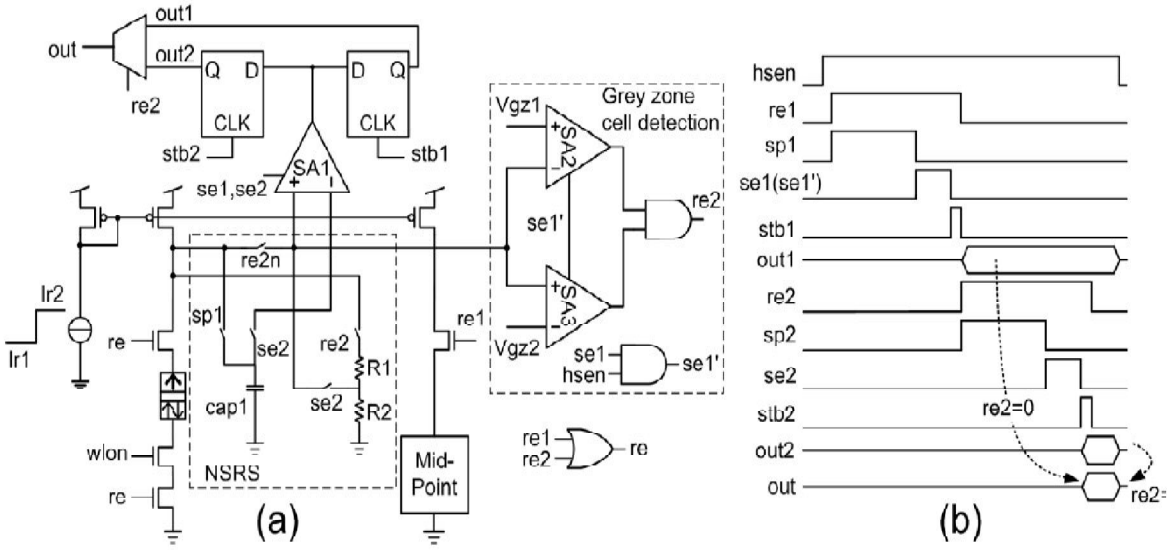

Fig.2. (a) Schematic and (b) timing diagram of the proposed hybrid sensing scheme.

In this work, a hybrid sensing scheme with combined features from the conventional mid-point reference sensing and the NSRS is proposed. The scheme activates the NSRS when a STT-MRAM cell is detected to fall within the resistance overlapping grey zone (GZ) obtainablethrough accurate on-chip characterization technique [16]. The proposed scheme offer greatly reduced bit error rate (BER) over the mid-point sensing scheme while maintaining the option of higher operation speed when needed.

II. PROPOSED HYBRID SENSING SCHEME

Fig. 2(a) shows the schematic of a voltage mode hybrid sensing circuit which consists of the conventional mid-point sensing function, the non-destructive self-reference sensing (NSRS) function and the grey zone cell (GZC) detection function. As shown in Fig. 2(b), when hybrid sensing is enabled by activating hsen, one complete read operation consists of two read cycles. In the first read cycle the mid-point reference sensing is performed when a read current I_{r1} is steered into the cell branch and the mid-point reference branch by a PMOS current mirror pair. The NMOS transistor controlled by wlon activates the targeted memory cell. The voltage drops of the two branches are developed at the inputs of the sense amplifier (SA) SA1. The first voltage drop at the positive input of SA1 is sampled by the switch controlled by sp1 and stored onto a capacitor, cap1. Subsequently, se1 activates SA1 and produce the first output out1 which is captured by a D-type flip-flop. At the same time, se1' activates SA2 and SA3 which compare the read voltage of the MRAM cell with the two boundary voltages V_{gz1} and V_{gz2} of the grey zone, respectively. If the cell's resistance falls within the grey zone, re2 will be enabled and the second read cycle begins. In the second read cycle, a higher read current I_{r2} is sourced into the branch of the MRAM cell while the other branch is turned off. The switch controlled by re2 connects the active branch to a resistance divider network of R1 and R2 which scales the second voltage drop [15]. Subsequently, se2 is activated and the two corresponding switches connect the scaled second voltage drop and the stored first voltage drop to the positive and negative inputs of SA1. The second read output out2 is then obtained and stored in the other D-type flip-flop. The multiplexer at the output stage decides the final read output according to re2. If re2 is '0', out1will be sent out; otherwise out2 will be the final output.

The proposed hybrid sensing method combines the high speed of the mid-point sensing method and the tolerance to process variation in the non-destructive self-reference sensing method leveraging on the knowledge of device distribution characteristics. If the MRAM process is well controlled with tight resistance distributions with clear separation between the two resistance states, few, if not none, MRAM cells will fall inside the grey zone. Then hybrid sensing does not have to be activated. Simple ECC scheme can correct the few occurrences of read errors. On the other hand, when resistance overlapping is inevitable, hybrid sensing is activated to improve the raw BER before the use of ECC to further enhance the read reliability.

III. RESULTS AND DISCUSSION

The capability in reducing the BER of the proposed sensing method is evaluated in 0.18 □m technology using Monte-Carlo (MC) simulation with a Verilog-A perpendicular MTJ model. The effects of key process parameters variation such as MTJ diameter d_{MTJ}, tunneling barrier thickness t_{MgO} and

free layer thickness t_f on MTJ resistance distribution are modeled. RA and TMR of MTJ are defined as electrical parameters with values of 8.72 Ω·□m^2 and 85%. The nominal values for d_{MTJ}, t_{MgO} and t_f are 64.5, 1, and 1.9 nm, respectively. In our simulation, the standard variations □ of t_{ox} and t_f are set at 1% while the□□□of d_{MTJ} is set at 5%, 8% and 10% of their nominal values. Four pairs of read currents (I_{r1}-I_{r2}) of (15-25□A), (20-25□A), (20-30□A) and (25-30□A), respectively, are defined to evaluate the read energy of the proposed scheme. The total sample size of 1000 is used in all MC simulations.

Fig. 3 shows a comparison in BER between the hybrid scheme and the mid-point scheme across the process and read current corners. It can be observed the hybrid scheme is able to achieve at least 42.3% reduction in the raw BER across all defined corner.

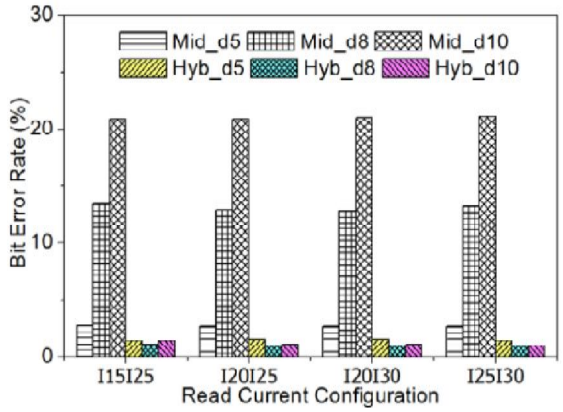

Fig. 3. Bit error rate improvement of the hybrid sensing over the mid-point sensing at three process variation corners across four read current configurations.

Unlike in the mid-point sensing method where BER increases tremendously with increasing process variation, the BER of the hybrid sensing method is not affected by the process variation due to the higher tolerance to process variation of the NSRS. Thus, the reduction in BER becomes very effective under high process variations. Read current configuration does not affect the BER in the hybrid sensing method either.

The read error in hybrid sensing can be further classified into two types. Type 1 (T1) is the NSRS read error of the second read cycle while cells having Type 2 (T2) error are misclassified to be out of the grey zone while having a mid-point read error. T1 error is related to the difference in slope of the voltage/current dependent resistance roll-off between the high and low resistance states, and is beyond the scope of this paper therefore it is treated as hard error. T2 error is soft error and can be suppressed. As shown in Fig. 4, T2 error dominates the read error in the proposed scheme, while only 1 count of T1 error occurred under the simulation condition of □□d_{MTJ}) □ 10% and read current pair of (15 □A, 25 □A). Although at □□d_{MTJ}) □ 5% resistance distribution at both resistance states is tighter than the other two values, the corresponding T2 error count is higher. This is resulted from the higher cell count within the minimum sensing zones of SA2 and SA3 due to denser cell distribution in the read voltage domain.

Fig. 5 shows a detailed read energy breakdown of the hybrid read cycle. Average read energy of the three main processes, the first mid-point read, the GZC detection and the second NSRS read over the read operations of '1' and '0' is plotted. It can be observed that among the three processes, GZC detection dissipates the most energy followed by the mid-point read and NSRS read. The GZC detection and the mid-point read operation are both unconditional processes. The GZC detection is performed using two sense amplifiers, thus the total energy dissipation is almost double the mid-point read operation. On the other hand, the NSRS read operation is a conditional process activated only when a cell is determined to fall within the GZ. The energy consumed by the NSRS read operation is dependent on the process variation which determines the total number of cells that require the NSRS read. Energy dependency on read current configuration is weak as the sense margin of NSRS read is related to the resistance roll-off slope. As process variation increases, resistance distribution broadens and the separation between the high and low resistance profiles decreases which results in smaller sense marge of SA1, SA2 and SA3.

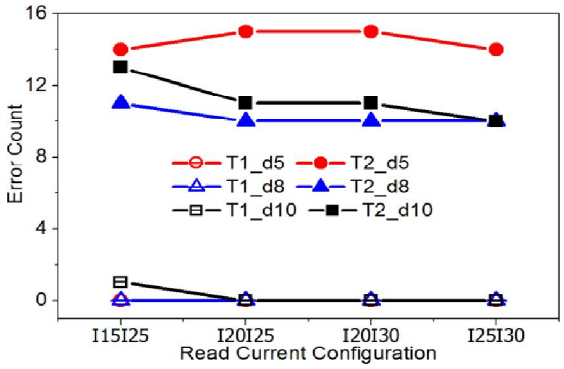

Fig. 4. The number of Type 1 (T1) and Type 2 (T2) errors in the 1000 MC simulation runs of the hybrid sensing scheme across the design corners.

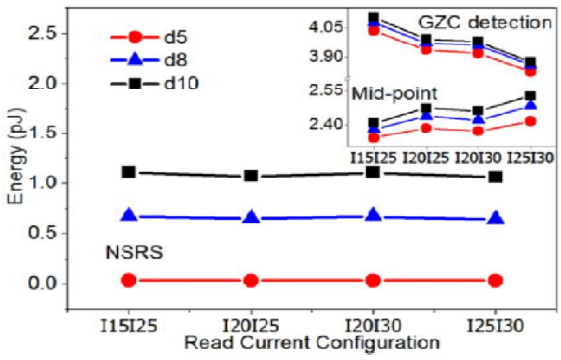

Fig. 5. Read energy dissipation breakdown of the hybrid sensing scheme.

The three sense amplifiers involved in the mid-point read and GZC detection operation require longer time to compare two inputs. This leads to higher energy dissipation with higher process variations. Besides, the energy dissipation of the two operations is dependent on the first read current value as higher read current will increase total DC current of the SA.

As mentioned previously, T2 error is soft error and can be suppressed by tuning the grey zone detection boundaries. By extending the GZ detection range wider than the actual characterized overlapping zone range, cells with T2 error in the original GZ condition (Fig. 4) will go through the low-error NSRS read operation. Cells that fall within the minimum sensing zone of the GZ SAs with the extended GZ range are further away from the mid-point reference. Even if some of them are incorrectly identified and skip the NSRS, their read output based on mid-point read operation will produce lower read error, as compared to the one with original GZ range. In the simulation setup, the grey zone range of all process variation corners were extended by 5 mV on both ends. Result shows that T2 error count has been reduced by at least 8 cells across process and design corners. As a result, the maximum total BER is reduced to 0.3% for the sample size of 1000. On average, 91.3%, 87.7% and 82.3% BER reduction was achieved for $\pm 1\sigma d_{MTJ}$) equal 5%, 8% and 10%, respectively, as compared to the one with the original GZ. The total read energy increases as larger number of cells go through the extra NSRS read, with a maximum increase of 6.9% across all the design corners. Overall, the extended GZ range lowers the BER greatly with a small energy overhead.

CONCLUSION

A hybrid sensing scheme leveraging on the speed advantage of mid-point reference sensing and process variation tolerance of the NSRS sensing was proposed in this paper. The sensing scheme can be configured to the mid-point reference sensing when the MRAM process variation is well controlled with tight resistance distribution and clear separation between the two resistance states. On the contrary, NSRS sensing is activated on cells whose resistance value fall within the resistance distribution overlapping zone (or grey zone). The sensing output taps on the mid-point sensing for cells outside of the grey zone and the NSRS sensing for cells within the grey zone. The proposed scheme achieves at least 42.3% reduction in BER over the typical mid-point reference sensing across MRAM process variation and read current corners. With an extended grey zone cell detection range, BER can be further reduced by 78.6% over the actual overlapping range. Offering a greatly improved BER under MRAM process variation, the proposed scheme is ideal for high reliability applications.

ACKNOWLEDGMENT

This work was supported by the Science and Engineering Research Council of A*STAR (Agency for Science, Technology and Research) Singapore, under Grant No.A1687b0033.

REFERENCES

[1] S. Fujita, H. Noguchi, K. Nomura, K. Abe, E. Kitagawa, N. Shimomura, and J. Ito, “Novel nonvolatile L1/L2/L3 cache memory hierarchy using nonvolatile-SRAM with voltage-induced magnetization switching and ultra low-write-energy MTJ,” IEEE Trans. Magn., vol. 49, no. 7, pp. 44–56, July 2013.

[2] G. Jan, L. Thomas, S. Le, Y.-J. Lee, H. Liu, J. Zhu, R.-Y. Tong, K. Pi, Y.-J. Wang, D. Shen, R. He, J. Haq, J. Teng, V. Lam, K. Huang, T. Zhong, T. Torng, and P.-K. Wang, “Demonstration of fully functional 8Mb perpendicular STT-MRAM chips with sub-5 ns writing for non-volatile embedded memories,” in Proc. Symp. VLSI Technol. Dig. Tech. Papers, Honolulu, USA, 2014, pp. 50–51.

[3] S. H. Kang, “Embedded STT-MRAM for energy-efficient and cost effective mobile systems,” in Proc. Symp. VLSI Technol.Dig. Tech. Papers, Honolulu, USA, 2014, pp. 44–45.

[4] S. Ikeda, K. Miura, H. Yamamoto, K. Mizunuma, H. D. Gan, M. Endo, S. Kanai, J. Hayakawa, F. Matsukura, and H. Ohno, “A perpendicular anisotropy CoFeB–MgO magnetic tunnel junction,” Nat. Mater., vol. 9, no. 9, pp. 721–724, 2010.

[5] D. C. Worledge, G. Hu, D. W. Abraham, J. Z. Sun, P. L. Trouilloud, J. Nowak, S. Brown, M. C. Gaidis, E. J. O’Sullivan, and R. P. Robertazzi, “Spin torque switching of perpendicular Ta|CoFeB|MgO-based magnetic tunnel junctions,” Appl. Phys. Lett., vol. 98, no. 2, pp. 022501, 2011.

[6] H. Noguchi, K. Ikegami, N. Shimomura, T. Tetsufumi, J. Ito, and S. Fujita, “Highly reliable and low-power non-volatile cache memory with advanced perpendicular STT-MRAM for high-performance cpu,” in Proc. Symp. VLSI Technol. Dig. Tech. Papers, Honolulu, USA, 2014, pp. 120–121.

[7] S. -W. Chung, T. Kishi, J. W. Park, M. Yoshikawa, K. S. Park, T. Nagase, K. Sunouchi, H. Kanaya, G. C. Kim, K. Noma, M. S. Lee, A. Yamamoto, K. M. Rho, K. Tsuchida, S. J. Chung, J. Y. Yi, H. S. Kim, Y. S. Chun, H. Oyamatsu, and S. J. Hong, “4Gbit density STT-MRAM using perpendicular MTJ realized with compact cell structure,” in Proc. IEEE IEDM Dig. Tech. Papers, San Francisco, CA, USA, 2016, pp. 27.1.1–27.1.4.

[8] Y. J. Song, J. H. Lee, H. C. Shin, K. H. Lee, K. Suh, J. R. Kang, S. S. Pyo, H. T. Jung, S. H. Hwang, G. H. Koh, S. C. Oh, S. O. Park, J. K. Kim, J. C. Park, J. Kim, K. H. Hwang, G. T. Jeong, K. P. Lee, and E. S. Jung, “Highly functional and reliable 8Mb STT-MRAM embedded in 28nm logic,” in Proc. IEEE IEDM Dig. Tech. Papers, San Francisco, CA, USA, 2016, pp. 27.2.1–27.2.2.

[9] X. Fong, S. Gupta, N. Mojunder, S. Choday, C. Augustine, and K. Roy, “KNACK: a hybrid spin-charge mixed-mode simulator for evaluating different genres of spin-transfer torque MRAM bit-cells,” in Proc. Int. Conf. Simulation Semiconductor Process. Devices(SISPAD), Osaka, Japan, 2011,pp. 51–54.

[10] G. Kil, J. Choi, and Y. Song, “Macro model for stochastic behavior of resistance distribution of magnetic tunnel junction,” Jpn. J. Appl. Phys., vol. 54, p. 04DD12, 2015.

[11] M. Gajek, J. J. Nowak, J. Z. Sun, P. L. Trouilloud, E. J.

O'Sullivan, D.W. Abraham, M. C. Gaidis, G. Hu, S. Brown, Y. Zhu, R. P. Robertazzi, W. J. Gallagher, and D. C. Worledge, "Spin torque switching of 20 nm magnetic tunnel junctions with perpendicular anistropy," Appl. Phys. Lett., vol. 100, p. 132408, 2012.

[12] K. L. Chun, H. Zhao, J. D. Harms, T. H. Kim, J. P. Wang, and C. H. Kim, "A scaling roadmap and performance evaluation of in-plane and perpendicular MTJ based STT-MRAMs for high-density cache memory," IEEE J. Solid-State Circuits, vol. 48, no. 2, pp. 598□610.

[13] T. Min, Z. Tokei, G. S. Kar, S. Coseman, J. Bekaert, P. Raghavan, S. Cornelissen, K. Xu, L. Souriau, D. Radisic, J. Swerts, T. Tahmasebi, and S. Mertens, "Interconnects scaling challenge for sub-20nm spin torque transfer magnetic random access memory technology," in Interconnect Tech. Conf. / Adv. Metallization Conf. (IITC/AMC), San Jose, USA, 2014, pp.341□344.

[14] C. W. Chien, D. Y. Wang, K. H. Shen, S. H. Huang, K. M. Kuo, S. Y. Yang, Y. H. Wang, T. K. Ku, and D. L. Deng, "Evidence of reactive-ion-etching-induced damages to the ferrormagnet of perpendicular magnetic tunnel junctions," IEEE Electron Device Lett., vol. 34, no. 2, pp. 241□243, 2013.

[15] Y. Chen, H. Li, X. Wang, W. Zhu, W. Xu, and T. Zhang, "A 130 nm 1.2 V/3.3 V 16 Kb STTMRAM with nondestructive self-reference sensing scheme," IEEE J. Solid-State Circuits, vol. 47, no. 2, pp. 560□573, 2012.

[16] F. Li, S. Y. H. Lua, and A. Mani, "An optimized resistance characterization technique for the next generation magnetic random access memory," IEEE Trans. Nanotechnology, vol. 14, no. 3, p. 540□545, 2015.

★★★